applied sciences

MDPI

Article

Research on a Dynamic Calibration Method for Photogrammetry Based on Rotary Motion

Jia Ou [1,2], Tingfa Xu [1,*], Xiaochuan Gan [3], Xuejun He [3], Yan Li [3], Jiansu Qu [3] and Wei Zhang [3]

[1] School of Optics and Photonics, Beijing Institute of Technology, Beijing 100081, China
[2] Chinese Aeronautical Establishment, Beijing 100029, China
[3] Beijing Changcheng Institute of Metrology and Measurement, Beijing 100095, China
* Correspondence: ciom_xtf1@bit.edu.cn

Abstract: Photogrammetry as an engineering measurement technology for the rapid and non-contact acquisition of geometric parameters, such as the attitude, position, and shape of a measured object, is widely used in the development and production processes of the aerospace and automobile industries. The calibration of a corresponding photogrammetry system is the basis for ensuring the accuracy of photogrammetry. The dynamic and static calibration of existing photogrammetry systems has not yet established a system calibration specification or standard, and such calibration has mainly focused on the internal and external parameters of the camera used in a photogrammetry system. The calibration of static parameters cannot fully guarantee the dynamic performance of a photogrammetry system in the process of measuring dynamic targets or micro-deformations. Aiming at the problem of dynamic parameter calibration of photogrammetry systems, this paper proposes a dynamic calibration method based on a circular trajectory standard device, which can realize the calibration of parameters, such as dynamic length measurement error, and ensure an accurate evaluation of the dynamic measurement performance of photogrammetry systems.

Keywords: dynamic parameter calibration; circle track; photography system; rotary motion

Citation: Ou, J.; Xu, T.; Gan, X.; He, X.; Li, Y.; Qu, J.; Zhang, W. Research on a Dynamic Calibration Method for Photogrammetry Based on Rotary Motion. *Appl. Sci.* **2023**, *13*, 3317. https://doi.org/10.3390/app13053317

Academic Editor: Mauro Lo Brutto

Received: 13 February 2023
Revised: 27 February 2023
Accepted: 1 March 2023
Published: 5 March 2023

1. Introduction

Photogrammetry is used to calculate the three-dimensional coordinates of space points through the principle of space intersection. With the help of high-precision cameras and fast image processors, photogrammetry can realize real-time measurement and monitoring of multiple points to calculate the attitude and position of a measured object and its shape change, as well as to realize real-time measurement and monitoring of multiple points. Dynamic photogrammetry [1–3] often adopts a double- or multiple-camera photogrammetry system [4] or a high-speed dynamic photogrammetry system to realize real-time calculation of dynamic geometric parameters. Among existing systems, the commonly used double- or multiple-camera photogrammetry system can usually reach a shooting frame rate of 1000 fps, perform online measurements of spatial three-dimensional coordinates of target points, and measure moving targets. In addition to providing temporal records of an object's space motion, such as deformation, trajectory, velocity, and acceleration curves, dynamic photogrammetry can also identify and image discrete target points. Therefore, dynamic photogrammetry has a wide range of applications in the fields of large component assembly in the aviation industry [5], crash testing in the automotive industry [6], dynamic deformation measurement during metal plate welding [7], calibration and evaluation of robot motion [8], measurement of real-scale heliostats [9], and human motion analysis [10]. For example, current civil aviation aircraft manufacturing adopts an international division of labor and cooperation mechanism. The major parts of an airframe are first produced and assembled by a manufacturer and then shipped to a final assembly plant. The assembly process of large parts involves real-time attitude adjustment and monitoring to realize the

complete assembly of parts. Through an accurate measurement and trimming of large-sized parts [11], it can avoid excessive clearance in the assembly process caused by dimensional deviation during assembly, which affects the overall performance of large equipment. As a typical large-scale measurement scene, the application of photogrammetry can build a spatial measurement coordinate system with minimum equipment investment and space consumption and realize the real-time measurement of spatial attitude and position [12].

As an engineering application technology widely used in large-scale measurement of space, photogrammetry is very important in terms of its measurement accuracy. At present, the calibration of a photogrammetry system mainly focuses on the calibration of static parameters, such as the internal and external parameters of the camera used in the system. Safouane et al. proposed an optimized calibration of a machine vision system based on machine learning, which is beneficial for detecting parts with a large volume [13]. Liu et al. proposed an integrated calibration technique based on rigorous modeling for a three-dimensional imaging system composed of a single camera and a wedge prism, which contributes to the recovery of any spatial object with geometric accuracy [14]. Static parameter calibration can ensure the accurate capture and expression of spatial position points, but it cannot guarantee the dynamic performance of a photogrammetry system. When a photogrammetry system is used for dynamic measurement, more attention should be paid to the accuracy of the geometric parameter measurement results in a dynamic environment [15–20]. For example, when calibrating the dynamic performance of a laser tracker [21–23], it is necessary to focus on evaluation parameters, such as dynamic speed limit, dynamic indication error, and dynamic indication variation.

This paper proposes a dynamic calibration method based on a circular trajectory standard device for the problem of dynamic parameter calibration of photogrammetry systems. The circular trajectory standard device can provide stable circular orbits of various rotational speeds; the photogrammetry system can take pictures of a measured target at a certain rotational speed, calculate the three-dimensional coordinates of the two marked points on the measured target, and finally realize the evaluation of the dynamic measurement performance of the photogrammetry system. The main contributions of this study are as follows:

(a) Based on the circular trajectory standard device, we propose a dynamic parameter calibration method, which can effectively realize the calibration of dynamic length measurement errors and other parameters.
(b) The design error of the calibration system is analyzed based on the motion characteristic of the circular trajectory device.
(c) The proposed method can provide a solution for the dynamic measurement performance evaluation of photogrammetry systems.

In Section 2, we introduce the proposed method, including the calibration system and its principle. In Section 3, we analyze the design error of the calibration system. In Section 4, we describe our experiments and analyze the experimental data. In Section 5, the uncertainty of the calibration system is calculated.

2. The Calibration Principle

The core principle of calibrating the dynamic parameters of a photogrammetry system is to provide a dynamic moving target with stable parameters and a unique spatial geometric conversion relationship. By comparing the measurement data of the photogrammetry system with the standard dynamic target design's motion parameters, the dynamic parameter calibration of the photogrammetry system is realized. Based on the above principles, Figure 1 shows the calibration device. The calibration system proposed in this paper consists of a control field, a circular trajectory standard device, and a binocular camera. The calibration field provides the standard spatial geometric relationship of a target point. Since internal parameters, such as the focal length of the camera, will change during the dynamic measurement process, a control field is introduced into the calibration system as a static reference plane for the dynamic calibration process. The stability of the control device

is very important [24,25]. The circular track-generating device in this study can generate a uniform circular motion of 0~1000 prm, in which the circular grating can provide the standard value of the speed for the standard device. Two targets with coding points are installed on a fixed position of the rotating rod. During the rotation process, the relative distance between the two coding points does not change, that is, the distance can be used as the standard value L during the experiment. Therefore, in the process of uniform rotation of the original trajectory-generating device, the binocular camera obtains the spatial coordinates of the two coding points in real time, calculates the distance L′ between the two coding points, and then compares it with the standard distance. The dynamic performance of the camera is then evaluated.

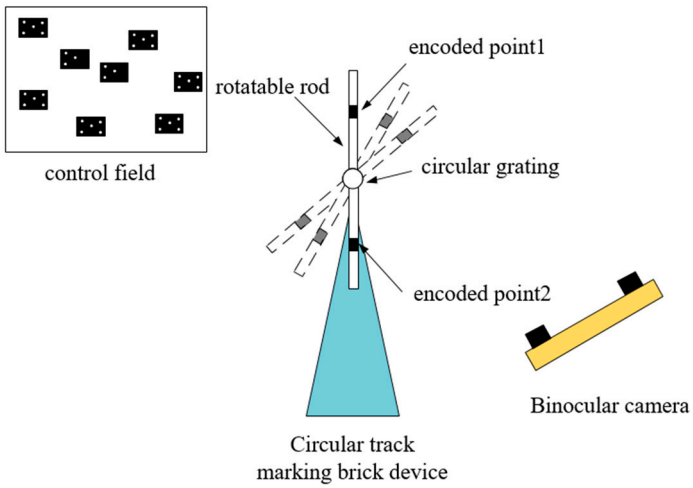

Figure 1. Calibration system's schematic diagram.

The control field consists of several photographic control points. These control points are the subjects of the digital photogrammetry system under test and are statically calibrated in advance to provide position criteria. These photographic control points are arranged on the machine and the wall around the turntable, which are relatively fixed and can be set as the fixed points in the calibration system. These photographic control points can also be used as a basis for calibration. According to the measuring range, these control points are often arranged, and the interval is generally between 200 mm and 500 mm.

The use of circular trajectories enables motion outputs with a large dynamic range. Even if the rotational speed does not change, by changing the radius, the linear speed of the dynamic target changes linearly. In addition, the stable control of speed is also a form of high-precision movement that can be achieved at present. The application of circular motion trajectory is not only a relatively optimized form to achieve the continuous and stable output of dynamic targets, but it is also the most convenient form of measurement value traceability.

3. Calibration System Design Error Analysis

The calibration system proposed in this paper mainly introduces dynamic motion parameters based on fixed target points to realize the calibration of dynamic parameters. Therefore, the measurement accuracy of the control field's marker point and the rotating rod's target point as a static and fixed relative position measurement is higher than that of static photogrammetric measurement by more than 10 times, and its influence on the dynamic parameter calibration can be ignored. Therefore, the circular trajectory generator is a key standard device for providing dynamic displacement in the circumferential direction, and its uniform rotational speed error directly affects the dynamic circular position.

For a uniform angular motion, the timed angle measurement method can be used to analyze the speed error, that is, to measure the angle that the turntable rotates in standard time. Alternatively, the fixed-angle timing method can be used, which measures

the time it takes for the turntable to rotate through a certain angle. The latter generally travels the distance in one cycle and evaluates the stability of the turntable in a short time. For the former method, the turntable usually rotates for several cycles, and relevant equipment, such as a frequency meter, is used to measure the elapsed time, which represents the stable performance of the turntable in a long time. Considering the sensitivity of the photogrammetry system calibration to the position accuracy, this paper adopts the fixed-angle time measurement method to calibrate and test the rotational speed error of the device.

There are space marks that are evenly distributed at the radius R = 500 mm of the disc installed on the turntable. When the photodetector passes through space, a high-level voltage signal will be generated, and the space between the marks is 10° ($\pi/18$). The turntable is set to create a constant speed circle at 25 rpm (2.6 rad/s), 50 rpm (5.2 rad/s), 100 rpm (10.5 rad/s), and 200 rpm (20.9 rad/s) at the same ratio, which is two times the speed range. For motion, the maximum rotational speed is calculated by measuring a value 1.2 times of the limit dynamic parameters of the photogrammetry system. The photodetector is used to record the rotational angle of the turntable, and the oscilloscope is used to record the waveform and time, as shown in Figures 2–5. The comparison data (the actual movement speed ω and the relative velocity error δ) between the different rotational speeds are shown in Table 1.

Table 1. The comparison data between different rotational speeds.

	n = 25 rpm	**n = 50 rpm**	**n = 100 rpm**	**n = 200 rpm**
ω	24.99 rpm	49.98 rpm	100.10 rpm	200.80 rpm
δ	0.04%	0.04%	0.10%	0.40%

(1) n = 25 rpm

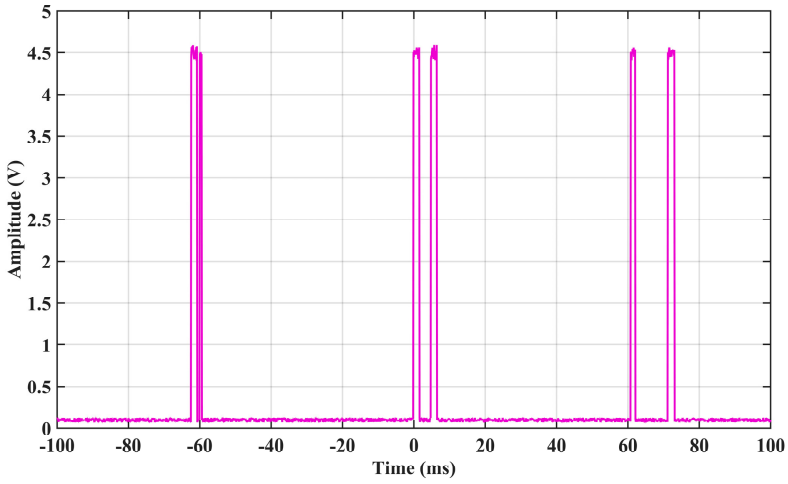

Figure 2. The 25 rpm oscilloscope waveform.

At 25 rpm, the actual movement speed of the turntable from the time and angle interval and the relative velocity error are calculated as follows:

$$\omega = \frac{\pi/18}{0.0667s} = 24.99 \text{ rpm}, \tag{1}$$

$$\delta = \frac{|25 - 24.99|}{25} \times 100\% = 0.04\%, \tag{2}$$

(2) n = 50 rpm

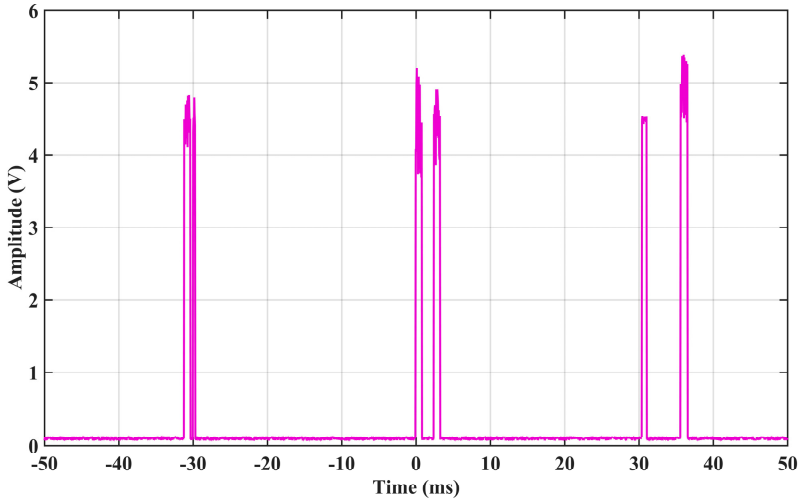

Figure 3. The 50 rpm oscilloscope waveform.

At 50 rpm, the actual movement speed of the turntable from the time and angle interval and the relative velocity error are calculated as follows:

$$\omega = \frac{\pi/18}{0.03335s} = 49.98 \text{ rpm}, \tag{3}$$

$$\delta = \frac{|50 - 49.98|}{50} \times 100\% = 0.04\%, \tag{4}$$

(3) n = 100 rpm

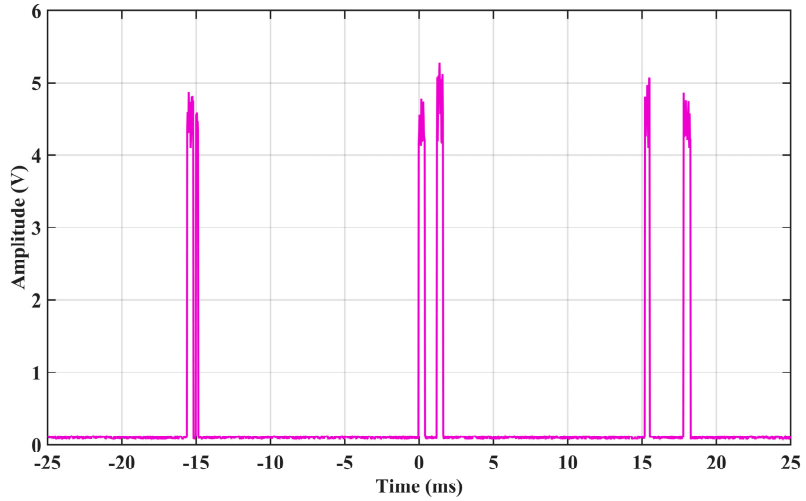

Figure 4. The 100 rpm oscilloscope waveform.

At 100 rpm, the actual movement speed of the turntable from the time and angle interval and the relative velocity error are calculated as follows:

$$\omega = \frac{\pi/18}{0.01665s} = 100.10 \text{ rpm}, \tag{5}$$

$$\delta = \frac{|100 - 100.10|}{100} \times 100\% = 0.10\%, \tag{6}$$

(4) n = 200 rpm

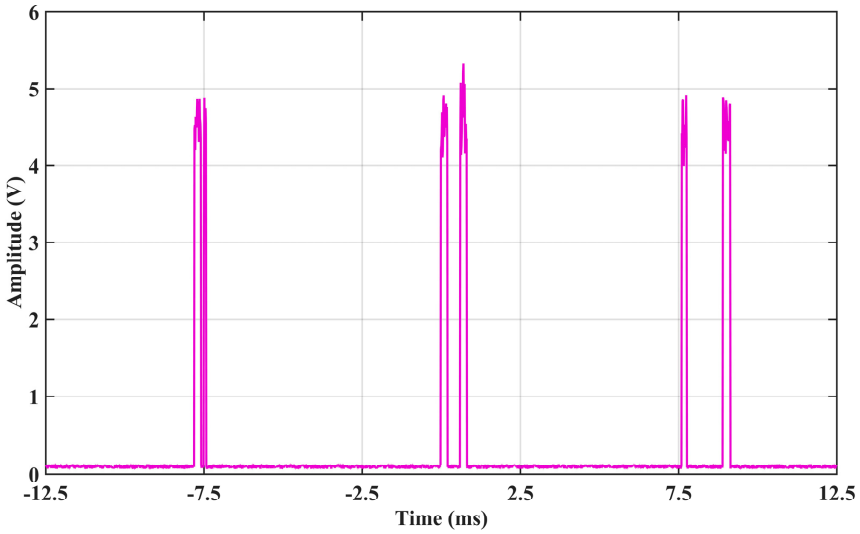

Figure 5. The 200 rpm oscilloscope waveform.

At 200 rpm, the actual movement speed of the turntable from the time and angle interval and the relative velocity error are calculated as follows:

$$\omega = \frac{\pi/18}{0.00830s} = 200.80 \text{ rpm}, \tag{7}$$

$$\delta = \frac{|200 - 200.80|}{200} \times 100\% = 0.40\%, \tag{8}$$

To sum up, it is evident from the actual measurement experiment that the relative rotational speed error of the circular trajectory-generating device is less than 0.1%, which meets the calibration requirements.

4. Experiment and Analysis

4.1. The Main Use Method of the Circumference Dynamic Calibration Device

(a) Measuring and controlling the field layout. The marking points suitable for calibrating the photogrammetry system are pasted on the device disc -LRB-; usually, the coding points are used for a quick tracking of the measuring system, and the marking points are the shooting objects of the measured digital photogrammetry system, which provides the location criteria through prior static calibration. The number of marks is two or more. The marks are pasted on the surface of the turntable with circular motion. When the turntable moves, the marks also maintains a corresponding movement. A sufficient number of marking points and control points are arranged around the turntable as the measuring control field, and at least one datum ruler is placed as the length datum.

(b) Measurement preparation of the photogrammetry system. Connect and arrange the camera, the controller, and the light source according to the system instruction. Additionally, according to the system operating instructions, the camera distance (recommended camera distance for the calibration device references a distance of 3 M), the camera distribution, and the rendezvous angle are selected. The system installation, layout, connection, and parameter setting are included. The field of view of the two cameras is aligned and held fixed at the middle position of the upper surface of the disc of the calibrated device. When the calibration device rotates, the photographic target is within the effective measuring range of the photogrammetry system.

(c) Dynamic calibration. Set the running speed of the dynamic calibration device, control the movement of the turntable, and use the calibrated photogrammetry system to

take continuous photographs of the moving photographic target. The position measurement results of the photogrammetry system at the corresponding velocity are obtained by processing and calculating the measurement using the software provided by the calibrated system.

(d) Result analysis. The measured results are compared with the standard values to verify the dynamic measurement performance of the digital photogrammetry system, including its length measurement error, motion trajectory, and velocity in a dynamic environment.

4.2. Circular Dynamic Parameter Calibration Test of Dual-Camera System

The calibration experiment of circular dynamic parameters was carried out using the Chenway® MPS/M10 dual-camera real-time industrial photogrammetry system (Chenway®, Tainan City, Taiwan). The circular track generator is placed in the measurement control field, which is composed of coding points and marker points, and two coding points are pasted on different positions of the rotating rod of the circular track generator. The number of coding points must not duplicate the code used in the control field. The circular trajectory generator's controller controls its rotational speed. After the rotating rod rotates at a certain speed, the dual-camera photogrammetry system tracks and measures the rotating target, and the maximum real-time measurement speed is four frames/second. Figure 6 shows the best site. To ensure the accuracy of the rotating rod in the working engineering and to minimize the real deformation of the rotating rod due to mechanical stress, the material of the rotating rod is made of high-hardness carbon fiber material; its outer diameter is 26 mm, and the wall thickness is 2 mm. The red frame on the left side of the small figure in Figure 6 represents the circular trajectory generator, and not the Chenwei's camera.

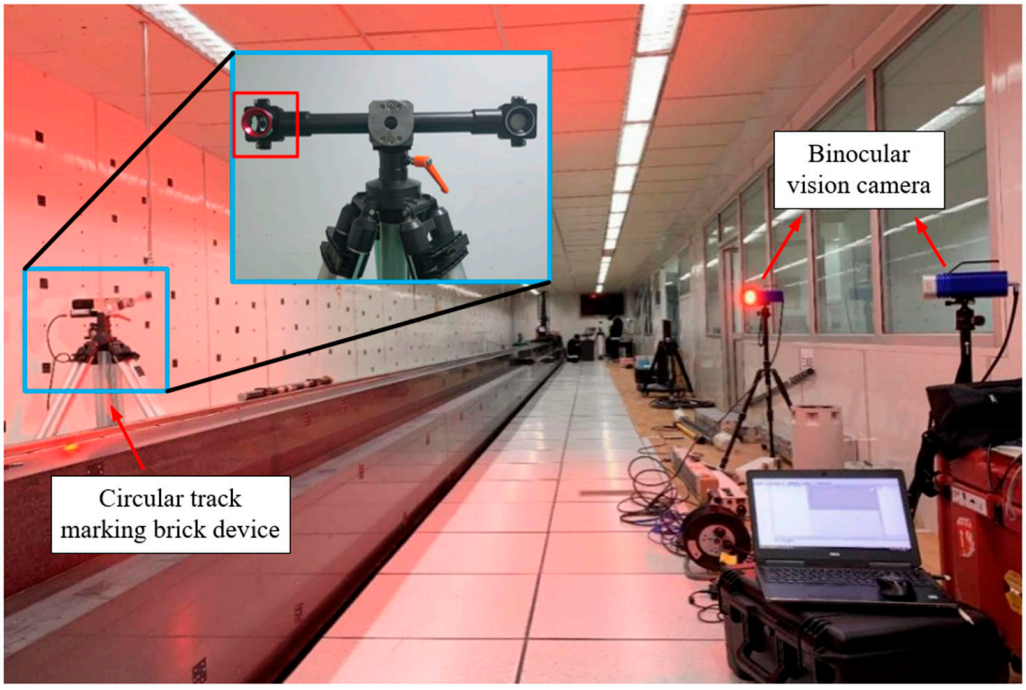

Figure 6. Circular dynamic parameter calibration test.

The main technical specifications of the Chenway® MPS/M10 dual-camera real-time industrial photogrammetry system (Chenway®, Tainan City, Taiwan). are summarized in Table 2.

Table 2. MPS/M10 technical specifications.

Technical Index	MPS/M10
Resolution ratio	8 M
Measuring accuracy	12 μm + 12 ppm·L 0.05 mm@3 m
Measurement accuracy of displacement and profile	0.03 mm@3 m
Field angle	70.6°
Measuring speed	Real-time processing of 5 frames/SEC; Post-processing of 10 frames per second
Measuring range	~15 m

4.3. Test Procedure

The main test steps are as follows (Figure 7):

(a) Connect the test equipment including the circular trajectory generator and the dual-camera real-time photogrammetry system.

(b) Camera calibration and control field calibration. Connect two cameras and calibrate them one by one. Turn on the laser indication of the camera. The operator, while holding the camera, stands about 3 m in front of the calibration field and points the camera at the center position of the calibration field at different positions at above and below, as well as left and right, of the calibration field (the camera pointing can be adjusted according to the laser indication) to take the calibration images. The number of images taken should not be less than 30; the position distribution in front of the calibration field should be basically even; and the images should be obtained from nine directions, and each direction is generally rotated four times around the optical axis of the camera, at 90° each time. After shooting, multiple images are used to solve the parameters in the camera and complete the camera calibration, as shown in Figure 8. Simultaneously, the control field is photographed with a camera to obtain the coordinates of each control point in the control field, as shown in Figure 9. The external parameter and the control field calibration data are then solved.

(c) Control field orientation. Install the two cameras on the tripod head, respectively; turn on the laser pointer, adjust the tripod or head; and adjust the pointing laser of the camera to the circular track generator. Use the measurement software to complete the control field orientation and determine the position of the two cameras.

(d) Dynamic measurement. Using the continuous measurement and deformation monitoring functions of the measuring system, two coding points on the rotating rod of the circular track are selected as the monitoring objects. The circular trajectory generator's controller controls the rotational speed, so that after the rotation rod rotates at a certain speed, the dual-camera photogrammetry system tracks and measures the two coding points and records the coordinate changes of the two points.

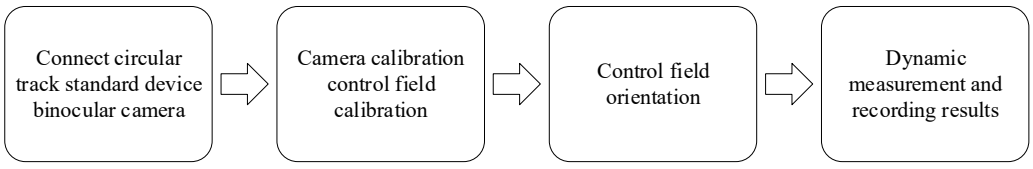

Figure 7. Experimental procedure.

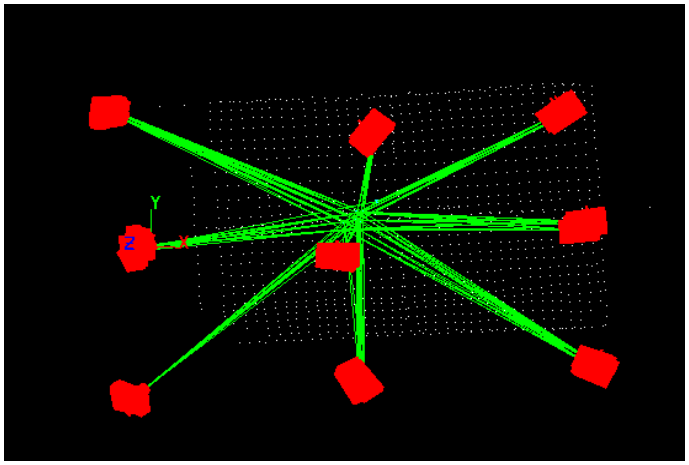

Figure 8. Camera calibration station's distribution map.

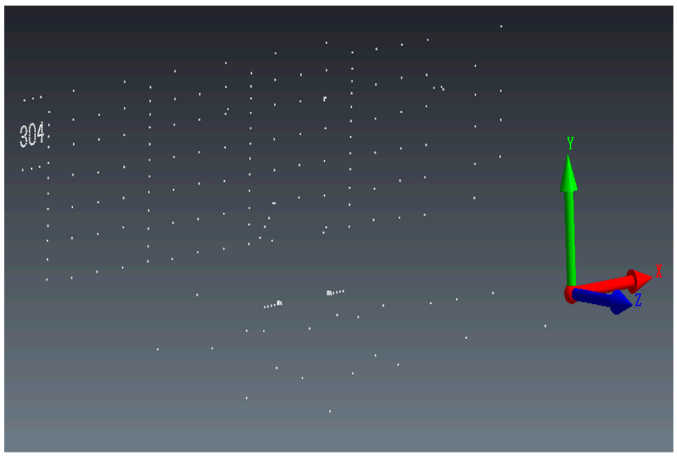

Figure 9. Test control field.

4.4. Test Data

The calculation results of the distance between two coding points at different speeds are as follows (shown in Figures 10–16):

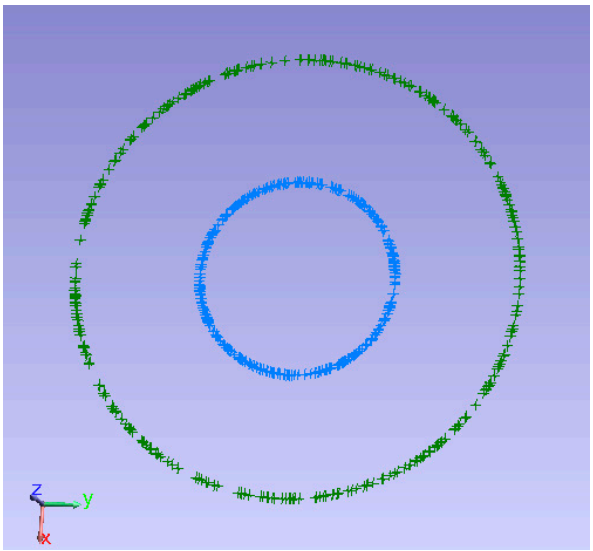

Figure 10. Circumferential dynamic test's target point trajectory.

(1) Speed R = 0 (static)

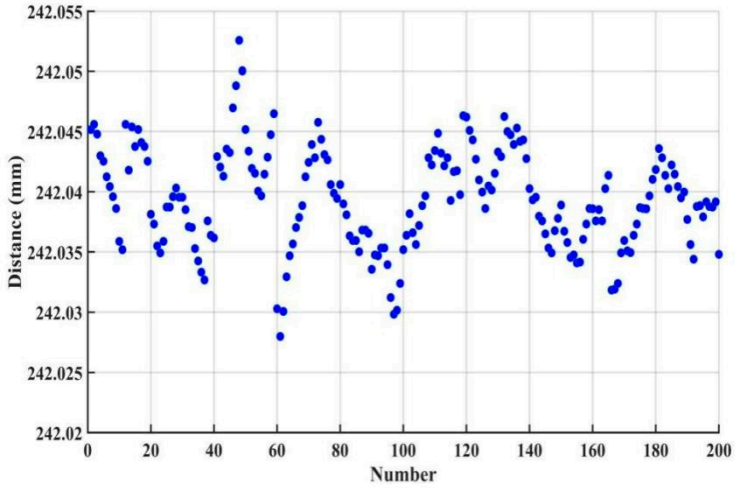

Figure 11. Measurement results of the distance between two targets in a stationary state.

(2) Speed R = 0.5 r/s

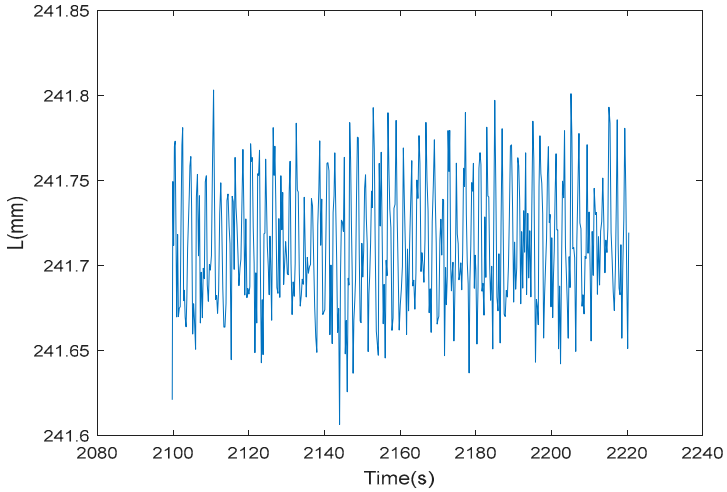

Figure 12. Measurement results of the distance between two targets at 0.5 r/s.

(3) Speed R = 1.0 r/s

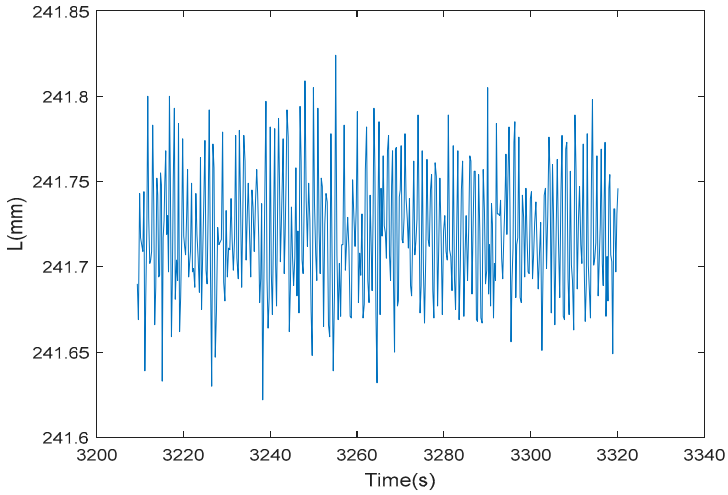

Figure 13. Measurement results of the distance between two targets at 1 r/s.

(4) Speed R = 2.0 r/s

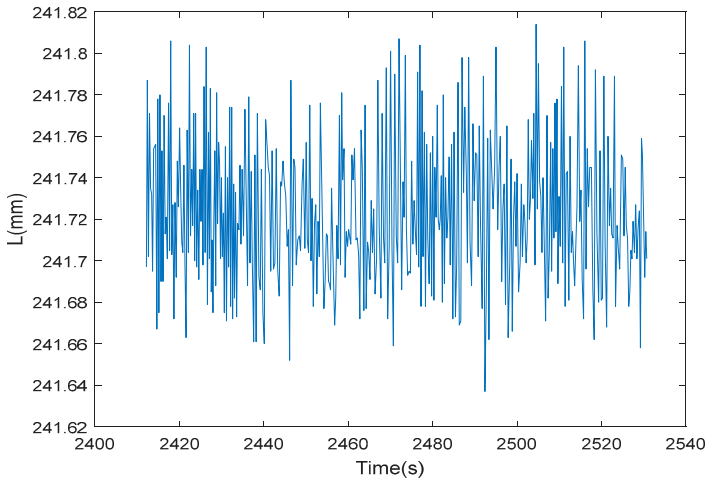

Figure 14. Measurement results of the distance between two targets at 2 r/s.

(5) Speed R = 3.0 r/s

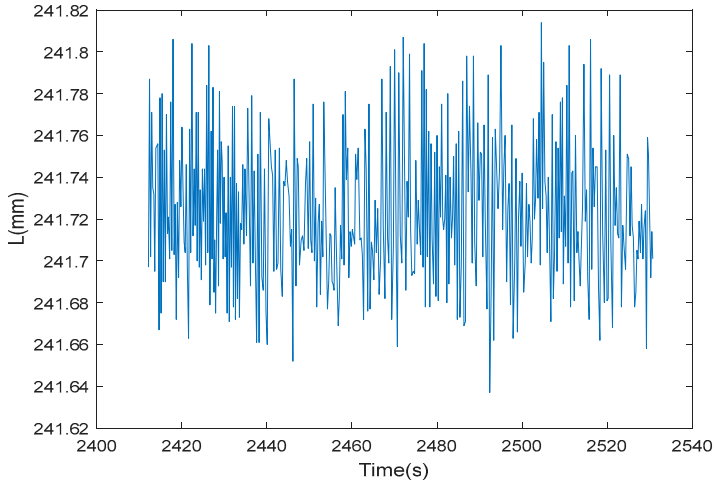

Figure 15. Measurement results of the distance between two targets at 3 r/s.

(6) Speed R = 4.0 r/s

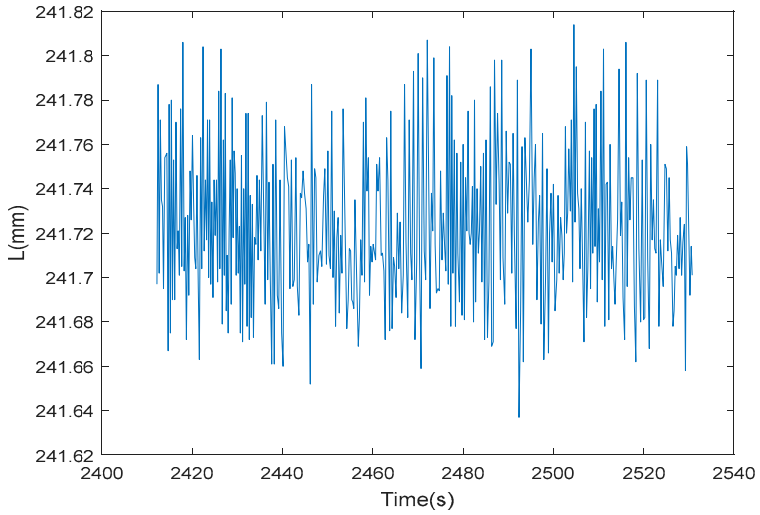

Figure 16. Measurement results of the distance between two targets at 4 r/s.

(7) The above experimental data statistics are as follows (shown in Table 3 and Figure 17):

Table 3. Measurement results of the distance between two targets at different speeds.

Speed (r/s)	Distance	
	Mean Value (mm)	Standard Deviation (mm)
0	242.039	0.004
0.5	241.712	0.037
1.0	241.720	0.038
2.0	241.723	0.036
3.0	241.727	0.035
4.0	241.725	0.035

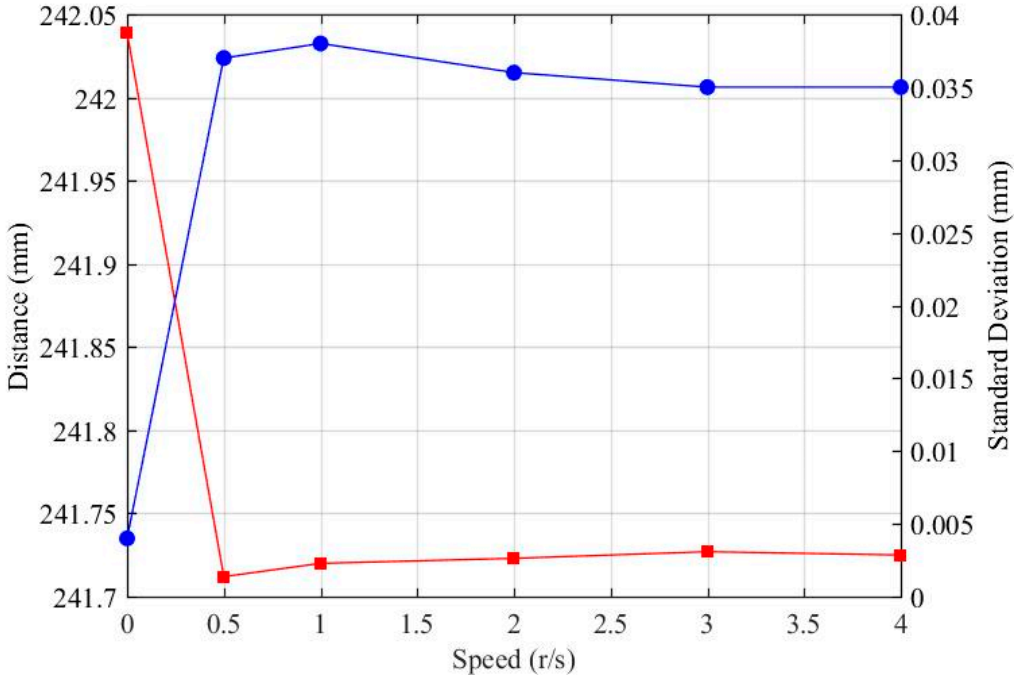

Figure 17. The relationship between the distance between two points and the rotational speed.

The moving speed of a target point can be calculated according to the spatial coordinates of the measured target point at a certain time and the time of image collection. About 400 frames of images are collected at each speed. The calculated results at different speeds are as follows (shown in Table 4):

(1) The amount of angle change represents the angle of rotation of the marker point relative to the previous position, and at the same time, the linear velocity and angular velocity in the table are all converted from this motion angle to time.

(2) The deviation in the Z direction can be understood as the amount of change in the direction of the motor axis of the target at the end of the swing arm during the rotation, and the change in this direction is perpendicular to the linear velocity direction at the end, so there is almost no effect.

Table 4. Calculation results at different speeds.

Rotate Speed (r/s)			Fitting Radius (mm)	Z to the Deviation (mm)	Angular Variation (°)	Linear Speed (mm/s)	Angular Speed (°/s)
0.5	Target point 1	mean value	167.970	0.000	45.837	524.420	178.883
		standard deviation	0.018	0.053	6.377	24.805	8.462
	Target point 2	mean value	73.745	0.000	45.837	230.238	178.883
		standard deviation	0.017	0.038	6.378	10.881	8.455
1.0	Target point 1	mean value	167.973	0.000	90.918	1053.511	359.355
		standard deviation	0.019	0.056	11.766	51.128	17.438
	Target point 2	mean value	73.751	0.000	90.918	462.558	359.354
		standard deviation	0.019	0.042	11.766	22.439	17.432
2.0	Target point 1	mean value	167.978	0.000	205.670	2112.440	720.536
		standard deviation	0.016	0.066	29.469	127.005	43.322
	Target point 2	mean value	73.749	0.000	203.754	924.852	718.518
		standard deviation	0.018	0.040	33.717	72.341	56.197
3.0	Target point 1	mean value	167.979	0.002	299.341	3167.066	1080.255
		standard deviation	0.017	0.075	49.143	163.237	55.691
	Target point 2	mean value	73.749	0.001	299.341	1390.462	1080.255
		standard deviation	0.017	0.047	49.142	71.676	55.691
4.0	Target point 1	mean value	167.981	0.000	313.244	3990.063	1360.949
		standard deviation	0.015	0.089	235.571	720.142	245.634
	Target point 2	mean value	73.747	0.000	308.932	1751.876	1361.078
		standard deviation	0.016	0.053	241.094	403.235	313.297

From the above data and analytical results, the following conclusions can be drawn:

(a) The radius of the circular trajectory of the target movement has no obvious relationship with the movement speed, and the difference does not exceed 10 μm. The experimental data are consistent with the relative position of the target point in the design of the device, and the error is mainly caused by the change in the verticality introduced by the rotating shaft system.

(b) The experimental data show that with an increase in the rotational speed, the RMS value of the circular trajectory fitting error increases to a certain extent, which indicates that the rotating motor selected for the calibration system has a certain rotary centrifugal error under high-speed motion. At the same time, the structure of the circular trajectory-generating device needs to be further strengthened to support its rigidity.

(c) When the two targets are in motion, the distance between the two points is calculated by the photogrammetry system, that is, the length decreases, and the decrease is about 0.2 mm. The decrease has no obvious relationship with the rotational speed, which is a system error. It is found that the reason for this phenomenon may be the shooting synchronization error between the two cameras of the binocular photogrammetry system, that is, there is a certain time difference in the shooting time of the two cameras for a dynamic target. In addition, when the target is in motion, the standard deviation of the distance between two points calculated by the photogrammetry system increases relative to the static state.

(d) When the rotational speed is less than 4.0 r/s, the speed value calculated by the photogrammetry system is consistent with the standard value, and the speed fluctuation

is within 8%. However, when the rotational speed is greater than 4.0 r/s, the real-time measurement frame rate of the photogrammetry system is about 4 frames/s, and there is a certain deviation in the interval time between two adjacent frames. Therefore, when the rotational angle of a target and the image acquisition time correspond to each other, errors are prone to occur, resulting in an error in the speed calculation, and the resulting error value is large. It shows that when the real-time measurement frame rate of the photogrammetry system is 4 frames/s, the maximum rotational speed of a target that can be accurately measured cannot exceed 4.0 r/s.

5. Calibration System Uncertainty Analysis

The measurement uncertainty analysis of the device includes the run-out uncertainty of the turntable, the error caused by the installation of the encoder, and the run-out error of the turntable caused by the table body. In theory, the points on the turntable should always move around a fixed axis, but the fact that the axis is in constant motion causes the points on the turntable to move in an irregular circle. The radial run-out can be ignored compared with the radius, so the resulting speed error for the turntable can be ignored. The measurement uncertainty analysis of the device is as follows:

(1) Uncertainty introduced by rotational consistency

The rotational speed error is calculated as the maximum error of 0.02% of the measured value, which is a uniform distribution estimation, and the introduced uncertainty component is calculated as follows:

$$u_1 = \frac{0.002\%}{\sqrt{3}} \approx 0.012\%, \tag{9}$$

(2) Uncertainty introduced by measurement repeatability

According to the measured data, the rotational speed is set to 600 r/min, and the corresponding introduction uncertainty is calculated as follows:

$$u_2 = \frac{0.01\%}{3} \approx 0.003\%, \tag{10}$$

(3) The change in the length perpendicular to the direction of rotation introduced by the rotating shaft system

An analysis of the change in the length perpendicular to the direction of rotation introduced by the rotation axis shows that the change is less than 0.1 mm, which is estimated based on a uniform distribution.

$$u_3 = \frac{0.1 \text{ mm}}{500 \text{ mm} \times \sqrt{3}} \times 100\% \approx 0.012\%, \tag{11}$$

(4) Relative standard uncertainty of synthesis

Regardless of the correlation between the above terms, the relative uncertainty of the synthesis is as follows:

$$u_{rel} = \sqrt{\sum_{i=1}^{8} u_i^2} \approx 0.017\%, \tag{12}$$

(5) Relative expansion uncertainty

If the inclusion factor $k = 2$ is used, the relative extension uncertainty is as follows:

$$U_{rel} = k u_{rel} \approx 0.03\% (k = 2), \tag{13}$$

6. Conclusions

In this paper, a photogrammetric dynamic parameter calibration method is proposed, and a calibration system is built. It is verified by the calibration experiments that the spatial dynamic parameter fitting method of the superimposed dynamic circular motion of static target points can achieve accurate expression of spatial dynamic position and meet the needs of dynamic calibration of photogrammetry systems. In the process of dynamic calibration of a photogrammetry system, the key to dynamic position fitting lies in the accuracy of circular motion parameters, and the accuracy of the rotational speed and shaft position is the main system errors. Simultaneously, the measurement frame rate of the measurement system should be fully considered during the calibration process to ensure that the sampling frequency of the relative position rotation is matched with it. The experimental results show that when the real-time measurement frame rate of the photogrammetry system is 4 frames/s, the maximum rotational speed of the target that can be accurately measured cannot exceed 4.0 rpm; in this state, the speed value calculated by the photogrammetry system is consistent with the standard value, and the speed fluctuation is within 8%.

Author Contributions: Conceptualization, J.O. and T.X.; Methodology, X.G. and W.Z.; Software, J.Q.; Validation, T.X. and X.H.; Formal analysis, J.O.; Investigation, X.G.; Resources, J.O.; Data curation, Y.L.; Writing—original draft, J.O.; Writing—review & editing, J.O.; Visualization, J.O.; Supervision, T.X. All authors have read and agreed to the published version of the manuscript.

Funding: This research received no external funding.

Institutional Review Board Statement: Not applicable.

Informed Consent Statement: Not applicable.

Data Availability Statement: Not applicable.

Conflicts of Interest: The authors declare no conflict of interest.

References

1. Van der Sluijs, J.; Kokelj, S.V.; Fraser, R.H.; Tunnicliffe, J.; Lacelle, D. Permafrost Terrain Dynamics and Infrastructure Impacts Revealed by UAV Photogrammetry and Thermal Imaging. *Remote Sens.* **2018**, *10*, 1734. [CrossRef]
2. Havaran, A.; Mahmoudi, M. Extracting structural dynamic properties utilizing close photogrammetry method. *Measurement* **2019**, *150*, 107092. [CrossRef]
3. Tang, H.Y.; Foo, H.C.Y.; Tan, I.S.; Lam, M.K. Photogrammetry based computational fluid dynamics of erosion of sand particles in water pipeline: Dynamic shape factors of 3D particles and minimization of erosion activity-ScienceDirect. *J. Pet. Sci. Eng.* **2021**, *205*, 108794. [CrossRef]
4. Wang, W.; Pan, W.; Hu, D.; Tang, G. Configuration optimization of photogrammetry system based on spectral radius for on-orbit measurement. *Trans. Inst. Meas. Control.* **2021**, *43*, 2483–2499. [CrossRef]
5. Zhao, G.; Zhang, C.; Jing, X.; Ling, X.; Chen, S. Study on the Technologies of Close Range Photogrammetry and Applications in the Manufacture of Aviation. In Proceedings of the 2018 8th International Conference on Manufacturing Science and Engineering (ICMSE 2018), Shenzhen, China, 30–31 March 2018.
6. Bish, J.; Caplinger, J.; Friedman, D.; Jordan, A.; Nash, C. Repeatability of a dynamic rollover test system. *Traffic Inj. Prev.* **2016**, *17*, 638–643.
7. Liu, J.W.; Liang, J.; Liang, X.H.; Tang, Z.Z. Videogrammetric system for dynamic deformation measurement during metal sheet welding processes. *Opt. Eng.* **2010**, *49*, 033601. [CrossRef]
8. Mcnamee, L.P. Photogrammetric Calibration of Mobile Robot Kinematics. Ph.D. Thesis, University of Ottawa, Ottawa, ON, Canada, 2003.
9. Blume, K.; Röger, M.; Schlichting, T.; Macke, A.; Pitz-Paal, R. Dynamic photogrammetry applied to a real scale heliostat: Insights into the wind-induced behavior and effects on the optical performance—ScienceDirect. *Sol. Energy* **2020**, *212*, 297–308. [CrossRef]
10. Kováts Jr, F.; Kiss, P.; Naszlady, A.; Nemeskéri, I. Morphometry of the Breathing Movements of the Trunk: A Dynamic, Double-view Photogrammetry Technic. In *Respiration*; Pergamon: Oxford, UK, 1981; pp. 55–56.
11. Alzahrani, F.; Hobiny, A.; Abbas, I.; Marin, M. An eigenvalues approach for a two-dimensional porous medium based upon weak, normal and strong thermal conductivities. *Symmetry* **2020**, *12*, 848. [CrossRef]
12. Scutaru, M.L.; Vlase, S.; Marin, M.; Modrea, A. New analytical method based on dynamic response of planar mechanical elastic systems. *Bound. Value Probl.* **2020**, *2020*, 1–16. [CrossRef]

13. El Ghazouali, S.; Vissiere, A.; Lafon, L.F.; Bouazizi, M.L.; Nouira, H. Optimised calibration of machine vision system for close range photogrammetry based on machine learning. *J. King Saud Univ. Comput. Inf. Sci.* **2022**, *34*, 7406–7418. [CrossRef]
14. Liu, X.; Li, A. An integrated calibration technique for variable-boresight three-dimensional imaging system. *Opt. Lasers Eng.* **2022**, *153*, 107005. [CrossRef]
15. Wan, A.; Song, L.; Xu, J.; Liu, S.; Chen, K. Calibration and compensation of machine tool volumetric error using a laser tracker. *Int. J. Mach. Tools Manuf.* **2018**, *124*, 126–133. [CrossRef]
16. Zhang, X.; Xu, Y.; Li, H.; Zhu, L.; Wang, X.; Li, W. Flexible method for accurate calibration of large-scale vision metrology system based on virtual 3-D targets and laser tracker. *Int. J. Adv. Robot. Syst.* **2019**, *16*, 172988141989351. [CrossRef]
17. Xu, P.; Cheung, B.C.; Li, B. A complete, continuous and minimal POE-based model for five-axis machine tools calibration with a single laser tracker, a R-test or a double ball-bar. *J. Manuf. Sci. Eng.* **2019**, *141*, 1. [CrossRef]
18. Morais, J.V.; Custódio, A.L.; Marques, G.M. Calibration of parameters in Dynamic Energy Budget models using Direct-Search methods. *J. Math. Biol.* **2019**, *78*, 1439–1458. [CrossRef] [PubMed]
19. González-Vera, A.S.; Wilting, T.J.S.; Holten, A.P.C.; van Heijst, G.J.F.; Duran-Matute, M. High-resolution single-camera photogrammetry: Incorporation of refraction at a fluid interface. *Exp. Fluids* **2020**, *61*, 1–19. [CrossRef]
20. Yusoff, I.N.; Ismail, M.A.M.; Tobe, H.; Miyoshi, T.; Date, K.; Yokota, Y. Discontinuity pattern detection and orientation measurement for tunnel faces by using structure from motion photogrammetry. *Displays* **2023**, *76*, 102356. [CrossRef]
21. Chen, Z.; Lai, J.; Liu, J.; Li, R.; Ji, G. A Parameter Self-Calibration Method for GNSS/INS Deeply Coupled Navigation Systems in Highly Dynamic Environments. *Sensors* **2018**, *18*, 2341. [CrossRef] [PubMed]
22. Mendikute, A.; Yagüe-Fabra, J.A.; Zatarain, M.; Bertelsen, Á.; Leizea, I. Self-Calibrated In-Process Photogrammetry for Large Raw Part Measurement and Alignment before Machining. *Sensors* **2017**, *17*, 2066. [CrossRef]
23. Wang, S.; Diao, R.; Xu, C.; Shi, D.; Wang, Z. On Multi-Event Co-Calibration of Dynamic Model Parameters Using Soft Actor-Critic. *IEEE Trans. Power Syst.* **2021**, *36*, 521–524. [CrossRef]
24. Brizuela-Mendoza, J.A.; Sorcia-Vázquez, F.D.; Rumbo-Morales, J.Y.; Lozoya-Ponce, R.E.; Rodríguez-Cerda, J.C. Active fault tolerant control based on eigenstructure assignment applied to a 3-DOF helicopter. *Asian J. Control.* **2021**, *23*, 673–684. [CrossRef]
25. Ortiz-Torres, G.; Castillo, P.; Sorcia-Vazquez, F.D.; Rumbo-Morales, J.Y.; Brizuela-Mendoza, J.A.; De La Cruz-Soto, J.; Martínez-García, M. Fault estimation and fault tolerant control strategies applied to VTOL aerial vehicles with soft and aggressive actuator faults. *IEEE Access* **2020**, *8*, 10649–10661. [CrossRef]